



Single-plane multiple speckle pattern phase retrieval using a deformable mirror

Almoro, Percival F.; Glückstad, Jesper; Hanson, Steen Grüner

Published in:
Optics Express

Link to article, DOI:
[10.1364/OE.18.019304](https://doi.org/10.1364/OE.18.019304)

Publication date:
2010

Document Version
Publisher's PDF, also known as Version of record

[Link back to DTU Orbit](#)

Citation (APA):
Almoro, P. F., Glückstad, J., & Hanson, S. G. (2010). Single-plane multiple speckle pattern phase retrieval using a deformable mirror. *Optics Express*, 18(18), 19304-19313. <https://doi.org/10.1364/OE.18.019304>

General rights

Copyright and moral rights for the publications made accessible in the public portal are retained by the authors and/or other copyright owners and it is a condition of accessing publications that users recognise and abide by the legal requirements associated with these rights.

- Users may download and print one copy of any publication from the public portal for the purpose of private study or research.
- You may not further distribute the material or use it for any profit-making activity or commercial gain
- You may freely distribute the URL identifying the publication in the public portal

If you believe that this document breaches copyright please contact us providing details, and we will remove access to the work immediately and investigate your claim.

Single-plane multiple speckle pattern phase retrieval using a deformable mirror

Percival F. Almoró,^{1,*} Jesper Glückstad,² and Steen G. Hanson²

¹*National Institute of Physics, University of the Philippines, Quezon City 1101, Philippines*

²*DTU Fotonik, Department of Photonics Engineering, Technical University of Denmark, DK-4000 Roskilde, Denmark*

**pfalmoro@gmail.com*

Abstract: A design for a single-plane multiple speckle pattern phase retrieval technique using a deformable mirror (DM) is analyzed within the formalism of complex ABCD-matrices, facilitating its use in conjunction with dynamic wavefronts. The variable focal length DM positioned at a Fourier plane of a lens comprises the adaptive optical (AO) system that replaces the time-consuming axial displacements in the conventional free-space multiple plane setup. Compared with a spatial light modulator, a DM has a smooth continuous surface which avoids pixelation, pixel cross-talk and non-planarity issues. The calculated distances for the proposed AO-system are evaluated experimentally using the conventional free-space phase retrieval setup. Two distance ranges are investigated depending on whether the measurement planes satisfy the Nyquist detector sampling condition or not. It is shown numerically and experimentally that speckle patterns measured at the non-Nyquist range still yield good reconstructions. A DM with a surface height of 25 microns and an aperture diameter of 5.2 mm may be used to reconstruct spherical phase patterns with 50-micron fringe spacing.

© 2010 Optical Society of America

OCIS codes: (010.7350) Wave-front sensing; (100.5070) Phase retrieval; (100.3010) Image reconstruction techniques; (030.6140) Speckle; (050.1960) Diffraction theory; (230.6120) Spatial light modulator.

References and links

1. G. J. Williams, M. A. Pfeifer, I. A. Vartanyants, and I. K. Robinson, "Three-dimensional imaging of microstructure in gold nanocrystals," *Phys. Rev. Lett.* **90**(17), 175501 (2003).
2. J. R. Fienup, J. C. Marron, T. J. Schulz, and J. H. Seldin, "Hubble Space Telescope characterized by using phase-retrieval algorithms," *Appl. Opt.* **32**(10), 1747–1767 (1993).
3. P. F. Almoró, G. Pedrini, A. Anand, W. Osten, and S. G. Hanson, "Interferometric evaluation of angular displacements using phase retrieval," *Opt. Lett.* **33**(18), 2041–2043 (2008).
4. P. F. Almoró, P. N. Gundu, and S. G. Hanson, "Numerical correction of aberrations via phase retrieval with speckle illumination," *Opt. Lett.* **34**(4), 521–523 (2009).
5. P. F. Almoró, G. Pedrini, F. Zhang, A. M. S. Maallo, A. Anand, P. N. Gundu, W. Wang, A. Asundi, W. Osten, and S. G. Hanson, "Fault-tolerant characterization of phase objects using a speckle-based phase retrieval technique," *Int. J. Optomech.* (to be published).
6. P. F. Almoró, G. Pedrini, P. N. Gundu, W. Osten, and S. G. Hanson, "Phase microscopy of technical and biological samples through random phase modulation with a diffuser," *Opt. Lett.* **35**(7), 1028–1030 (2010).
7. J. Glückstad, and D. Palima, "Generalised Phase Contrast: Applications in Optics and Photonics," Springer Series in Optical Sciences, Vol. 146, 310 pp (2009).
8. K. A. Nugent, "X-ray noninterferometric phase imaging: a unified picture," *J. Opt. Soc. Am. A* **24**(2), 536–547 (2007).
9. S. Yang, and H. Takajo, "Quantization error reduction in the measurement of Fourier intensity for phase retrieval," *Jpn. J. Appl. Phys.* **43**(No. 8B), 5747–5751 (2004).
10. W. O. Saxton, "Correction of artefacts in linear and nonlinear high resolution electron micrographs," *J. Microsc. Spectrosc. Electron.* **5**, 661–670 (1980).
11. D. L. Misell, "An examination of an iterative method for the solution of the phase problem in optics and electron optics," *J. Phys. D Appl. Phys.* **6**(18), 2200–2216 (1973).
12. E. Kirkland, "Improved high resolution image processing of bright field electron micrographs: I. Theory," *Ultramicroscopy* **15**(3), 151–172 (1984).

13. G. R. Brady, M. Guizar-Sicairos, and J. R. Fienup, "Optical wavefront measurement using phase retrieval with transverse translation diversity," *Opt. Express* **17**(2), 624–639 (2009).
14. J. M. Rodenburg, and H. M. L. Faulkner, "A phase retrieval algorithm for shifting illumination," *Appl. Phys. Lett.* **85**(20), 4795–4797 (2004).
15. G. Pedrini, W. Osten, and Y. Zhang, "Wave-front reconstruction from a sequence of interferograms recorded at different planes," *Opt. Lett.* **30**(8), 833–835 (2005).
16. R. W. Gerchberg, and W. O. Saxton, "A Practical Algorithm for the Determination of Phase from Image and Diffraction Plane Pictures," *Optik (Stuttg.)* **35**, 237–246 (1972).
17. N. Loomis, L. Waller, and G. Barbastathis, "High-Speed Phase Recovery Using Chromatic Transport of Intensity Computation in Graphics Processing Units," in *Digital Holography and Three-Dimensional Imaging*, OSA Technical Digest (CD) (Optical Society of America, 2010), paper JMA7.
18. Y. Ichihashi, H. Nakayama, T. Ito, N. Masuda, T. Shimobaba, A. Shiraki, and T. Sugie, "HORN-6 special-purpose clustered computing system for electroholography," *Opt. Express* **17**(16), 13895–13903 (2009).
19. L. Camacho, V. Micó, Z. Zalevsky, and J. García, "Quantitative phase microscopy using defocusing by means of a spatial light modulator," *Opt. Express* **18**(7), 6755–6766 (2010).
20. C. Falldorf, M. Agour, C. v. Kopylow, and R. B. Bergmann, "Phase retrieval by means of a spatial light modulator in the Fourier domain of an imaging system," *Appl. Opt.* **49**(10), 1826–1830 (2010).
21. C. Kohler, F. Zhang, and W. Osten, "Characterization of a spatial light modulator and its application in phase retrieval," *Appl. Opt.* **48**(20), 4003–4008 (2009).
22. F. Zhang, G. Pedrini, and W. Osten, "Phase retrieval of arbitrary complex-valued fields through aperture-plane modulation," *Phys. Rev. A* **75**(4), 043805 (2007).
23. C. López-Quesada, J. Andilla, and E. Martín-Badosa, "Correction of aberration in holographic optical tweezers using a Shack-Hartmann sensor," *Appl. Opt.* **48**(6), 1084–1090 (2009).
24. H. T. Yura, and S. G. Hanson, "Optical Beam Wave Propagation through Complex Optical Systems," *J. Opt. Soc. Am. A* **4**(10), 1931–1948 (1987).
25. A. M. S. Maallo, P. F. Almoró, and S. G. Hanson, "Quantization analysis of speckle intensity measurements for phase retrieval," *Appl. Opt.* (to be published).
26. http://en.wikipedia.org/wiki/Spread_spectrum

1. Introduction

Phase retrieval is a method of physically recording object field intensities followed by numerical processing to obtain the complete object wavefront. Phase retrieval is also an important field of study because of its applications within crystallography [1], analysis of telescope alignment [2], interferometry [3], aberration correction [4], characterization and recognition of phase objects [5], phase microscopy of technical and biological samples [6] and optical cryptography and wavefront engineering [7]. Phase retrieval techniques that use multiple intensity measurements have the benefit of signal redundancy and the advantage of being able to probe the signal at different sensitivity levels [8]. Compared to techniques that use a single intensity recording, methods that use multiple intensities are stable to noise, especially the noise introduced by detector quantization [9]. The approach of using multiple intensity measurements in iterative phase retrieval is not new. An early experimental demonstration of this approach is a study by Saxton [10] using electron micrographs with focus variation. Misell in [11] used a series of through-focus intensity measurements to enhance the convergence of the iterative phase calculation. Kirkland in [12] described a nonlinear imaging reconstruction algorithm by matching the electron-wave function to a series of measured defocused micrographs. Various modes of introducing phase diversity have also been employed in recently reported techniques including transverse translation of an aperture by Fienup, et al. [13], shifting illumination by Rodenburg and Faulkner [14], and detector translation at axially-displaced planes by Pedrini, et al. [15], to mention just a few. In our related works [3–6], we used a technique which is a variant of [15] in terms of the intensity measurements being carried out at axially-displaced planes. The main feature in our technique, however, is the use of a phase diffuser which, when illuminated with a coherent light, generates a partially-developed speckle field (PDSF) [3–6]. The spatial overlap of the scattered wave and unperturbed wave components of the PDSF facilitates for an enhanced axial intensity variation [3–6]. In iterative phase retrieval algorithms, it is known that a change in amplitude (square root of intensity) distribution alone at an input plane will result in changing both the amplitude and phase distributions at the output plane [16]. The axially-displaced intensity patterns of a PDSF provide more information about the change in the amplitude distribution than is available in regular diffraction patterns.

Figure 1(a) shows the conventional free-space recording setup for the speckle-based phase retrieval system [3–6] where the field intensity is measured at multiple planes separated by a distance Δz . The detector is being moved to a variable position L to sample the volume speckle field at each of the multiple planes (usually 20). Wavefront reconstruction is then carried out using an algorithm based on the angular spectrum method applied iteratively between the adjacent planes [3–6]. One possible drawback of the multiple-plane phase retrieval technique is the extended period of speckle recording (approximately one minute) due to the mechanical displacement of the detector, thus, restricting its application to purely static fields. It is remarked that the post processing time depends on the speckle array size. Decreasing the array size reduces the processing time significantly, to a few seconds per iteration, thus, allowing near real-time reconstructions. The use of very smaller arrays (for example, 200×200 pixels), however, may already have some effects on the wavefront resolution. Alternatively, the computing time may also be reduced by using a graphics processing unit because of the characteristic parallel architecture [17] or by using a cluster of computers [18].

In previous implementations of the technique [3–6], the position of the first measurement plane (Z_0) has been chosen to satisfy the well-known Nyquist sampling condition. The Nyquist condition dictates that the mean speckle size at the detector plane should be at least twice the width of the detector pixel. Positioning the detector far from the object increases the mean speckle size, thus, satisfying the sampling condition. Such large distances and the finite sensor area, however, decrease the effective numerical aperture and affect the resolution of the system. The Nyquist condition is especially critical for reconstruction methods that rely on a single intensity measurement like, for example, in the case of conventional off-axis digital holography. The carrier fringe spacing in the recorded off-axis hologram must be at least twice the width of the detector pixel in order to adequately represent the hologram fringes. For the case of the iterative reconstruction method which primarily utilizes the axial intensity variation in the multiple measurement planes [3–6,15], the remaining useful information, despite being obtained at a non-Nyquist distance range, may still facilitate for the reconstruction, hence, would be worth investigating.

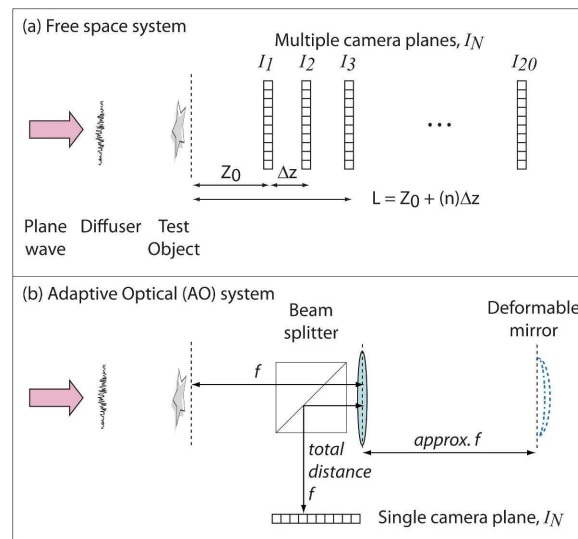


Fig. 1. (a) Setup for the conventional free-space multiple plane phase retrieval system. (b) Proposed setup based on an Adaptive Optical (AO) system using a deformable mirror.

A major improvement in the multiple-intensity phase retrieval technique [15] has been brought about by the embodiment of the phase diversity using an active optical device such as a spatial light modulator (SLM) [19–21]. In the microscopy setup in [19], phase diversity in the form of low lens defocus functions are displayed on an SLM that is positioned before a

tube lens. The series of positive and negative low lens defocus functions at the SLM facilitates intensity variation of the diffraction pattern at a fixed detector plane. The results obtained for the test object used via phase retrieval in [19] highly correlated with those obtained using the more-established digital holographic microscopy. In [20], the phase diversity is embodied by varying the distance parameter in the transfer function as displayed on the SLM that is positioned at the Fourier plane, playing the role of free-space propagation at the image plane. The successful reconstructions of speckle fields from rough objects in [20] make the phase retrieval technique a viable tool in coherent metrology and in nondestructive testing. The first-time use of SLM in the multiple-intensity phase retrieval approach was demonstrated by Kohler, et al. [21]. In [21], the SLM was used as a dynamic phase modulator to replace the transverse mechanical translation of a phase diffuser plate in a technique described in [22]. It was noted in [21] that such a high frequency diffuser function when displayed on the SLM appeared smoothed and spread out. These non-ideal modulation properties of the SLM and the cross-talk between pixels are partially alleviated by binning several adjoining pixels into a superpixel. This, on the other hand, results in a phase error in the form of a mosaic artefact [21]. In addition, the non-flatness of the SLM silicone backplane resulting in aberrations remains an intractable problem as reported in [23] and by the cited references therein.

In this study, we propose a new setup for the phase retrieval technique [3–6] based on a deformable mirror (DM) as the adaptive optical (AO) element which allows rapid measurements of the speckle patterns at a fixed detector plane. The advantages of using a DM are the smooth surface area and the large variation in the surface curvature. A theoretical model based on the ABCD matrix approach [24] describing the role of the AO element in the proposed technique is presented. It is emphasized that a phase diffuser plate is an integral part of the proposed setup, lending the technique especially adapted for low-curvature test wavefronts compared to, for example, the technique described in [19,20]. Without a diffuser plate in the path of such smooth wavefronts, the wave intensity may not vary significantly at the detector plane as the function that is displayed on the DM or SLM is varied. In addition, another benefit of the diffuser plate is the robustness against the various non-ideal modulation effects observed when using a random phase function on the SLM [21]. The rapid data acquisition offered by the proposed technique allows for the investigations of dynamic wavefronts. It also facilitates for a remote data processing over a network-connected hardware setup, for example, via the internet. Data acquisition is now often done in one station or laboratory and then transmitted to another, for example, as part of a collaborative research undertaking. Hence, rapid data acquisition with the proposed setup is imperative for the optimum utilization of any multiple-intensity reconstruction methods. The experimental issues involved in the implementation of the technique are also investigated numerically and experimentally using the conventional setup. The main focus of the experiments is to determine the effects of speckle recording at a non-Nyquist range or at distances wherein the mean speckle size is smaller than twice the detector pixel width. These short-range distances simulate the use of a DM with low surface curvature height. It is further remarked that surface imperfections in the DM, if any serious ones exist, may introduce aberrations in the retrieved phase maps. In such cases, numerical correction can be carried out using a calibration phase map [4].

Section 2 of this manuscript presents a theoretical evaluation of the proposed technique. The relations of the surface height and aperture diameter of the DM, as well as the focal length of the accessory lens on the effective distance are investigated. Section 3 shows sample calculations of the parameters for the physical realization of the proposed setup. Using a conventional free-space multiple plane setup, Sec. 4 presents the numerical and physical experiments aimed at evaluating the performance of the technique at different distances, specifically at distances that violate the Nyquist sampling condition. Finally, Sec. 5 gives the summary and the conclusions.

2. Theoretical evaluation of the optimal setup

The basic idea behind the concept is the almost simultaneous recording of speckle patterns corresponding to detecting at a plurality of axial positions. The allowable time within which all the recordings are made, is determined by the temporal decorrelation time of the disturbing medium or the movement of the object itself. In order to cope with the biologically most important examples, the optimal spatial modulation scheme has to be identified. There exists various ways of modulating an optical beam, of which SLM's used in beam projectors are the most well-known. But the use of a DM might be more desirable, as in our proposed setup, due to the lack of pixelation. The smooth continuous surface of a DM also avoids pixel cross-talk and the issue of non-planarity of the sensor substrate. The specifications of the DM, particularly the surface height and aperture size, and the focal length of the lens will be based on a theoretical evaluation. Using theoretically obtained values, laboratory experiments using the conventional free-space system will confirm the effectiveness of the proposed scheme. Besides, the basic trade-off between the spatial extent of the object plane and its resolution will have to be settled, as the space-bandwidth product of the system will be the limiting factor. For the acquisition of large data sets in the case of dynamic test objects, a fast scanning system may be used.

Figure 1(b) shows the embodiment of the proposed technique where the AO element (DM) has a focal length that goes from infinity to Δf . The comparison is done with respect to a free-space system in which the recording takes place at a (variable) distance of L . The system with the AO element consists of the following, which will be treated within the formalism of complex ABCD-matrices [24]:

- an object of diameter s_0 .
- free space propagation a distance f_1 .
- a lens with focal length f_1 .
- free space propagation a distance f_1 .
- a deformable mirror (the AO element) with a (variable) focal length Δf .
- with an aperture s_1 .
- free space propagation a distance f_2 .
- a lens with focal length f_2 .
- free space propagation a distance f_2 .
- free space propagation a distance Δz .

The relation between the field at the input- and output plane is given by

$$U_{out,x,y}(\mathbf{r}) = \int d\mathbf{r}' U_{in,x,y}(\mathbf{r}') G(\mathbf{r}', \mathbf{r}), \quad (1)$$

with the Green's function given by

$$G(\mathbf{r}', \mathbf{r}) = -\frac{ik}{2\pi B} \exp \left[-\frac{ik}{2B} (A\mathbf{r}'^2 - 2\mathbf{r}'\mathbf{r} + D\mathbf{r}^2) \right]. \quad (2)$$

In case of the basic free-space system, the matrix elements are:

$$M_{\text{freespace}} = \begin{Bmatrix} 1 - \frac{2iz}{ks_0^2} & z \\ -\frac{2iz}{ks_0^2} & 1 \end{Bmatrix} \quad (3)$$

where s_0 is the illumination spot size. In like manner, we obtain the matrix for the AO-system,

$$M_{AO} = \begin{pmatrix} -\frac{f_2}{f_1} + \frac{-4f_1f_2^2df + 2if_1(df dz + f_2^2)ks_1^2}{f_2k^2s_0^2s_1^2df} & -\frac{dzf_1}{f_2} + f_1f_2\left(\frac{1}{df} - \frac{2i}{ks_1^2}\right) \\ \frac{2if}{f_2ks_0^2} & -\frac{f_1}{f_2} \end{pmatrix} \quad (4)$$

The three parameters that are included in the Greens' function, Eq. (2), are A/B , $1/B$, and D/B . Here it is assumed that the AO-aperture and the incident beam are large, i.e., $s_1^2 \gg 2/(k\Delta f)$ and $s_0^2 \gg 2f_1^2/(k\Delta f)$. Table 1 shows a comparison of the three parameters for the AO system and the free space system.

Table 1. Parameters in the Green's function

Element	AO system	Free space
A/B	$\frac{f_2^2}{f_1^2} \frac{\Delta f}{\Delta f \Delta z + f_2^2}$	$\frac{1}{z}$
		$\frac{1}{z}$
1/B	$\frac{f_2}{f_1} \frac{\Delta f}{\Delta f \Delta z + f_2^2}$	$\frac{1}{z}$
		$\frac{1}{z}$
D/B	$\frac{\Delta f}{\Delta f \Delta z + f_2^2}$	$\frac{1}{z}$
		$\frac{1}{z}$

For the AO-system, we can write the Greens' function:

$$G(\mathbf{r}', \mathbf{r}) \propto \exp \left[-\frac{ik\Delta f}{2(\Delta f \Delta z + f_2^2)} \left(\frac{f_2}{f_1} \mathbf{r}' - \mathbf{r} \right)^2 \right]. \quad (5)$$

And for the free space system, we have:

$$G(\mathbf{r}', \mathbf{r}) \propto \exp \left[-\frac{ik}{2L} (\mathbf{r}' - \mathbf{r})^2 \right]. \quad (6)$$

A comparison of the two Greens' functions shows that the object is subject to a magnification of f_2 / f_1 . The effective- and variable – distance L_{eff} to the object in the AO-system is given by

$$L_{\text{eff}} = \frac{\Delta f \Delta z + f_2^2}{\Delta f}. \quad (7)$$

It is worth noting that Δf is proportional to the change in the radius of curvature of the AO-element. This means that Δf lies between infinity and a finite value. It will never attain a zero value. If we assume that the limiting value of Δf is infinity, then the change in effective distance to the object is

$$\Delta L_{eff} \equiv \frac{\Delta f \Delta z + f_2^2}{\Delta f} - \left(\frac{\Delta f \Delta z + f_2^2}{\Delta f} \right)_{\text{for } \Delta f \rightarrow \infty} = \frac{f_2^2}{\Delta f}. \quad (8)$$

3. Sample calculations

Here we calculate the effective distance at which the speckle field can be probed based on the effective change in the focal length of a DM. The aperture diameter (D) of the AO element is assumed to be 5.2 mm, and, when actuated, the surface height of the center of the diaphragm (h) goes from zero to 25 microns. It is remarked that the value of $h = 25$ microns used in this sample calculation is based on a typical specification for surface height of commercial DM's. Since the radius of curvature (R) is much greater than the surface height, i.e., $R \gg h$, we can use the approximation $R = (D/2)^2 / 2h$. This implies that R can vary between infinity and 135 mm. The focal length of the spherical mirror ($f = -R/2$), thus, varies between infinity and 68 mm. In Fig. 1(b), since the AO element is at the back focal plane of the accessory lens with focal length f , we have Δz in Eq. (7) equal to zero. If we compare the setup for an ordinary free space set up, L_{eff} will change between 0 and $f^2 / 68\text{mm}$. The effective distance can then be expressed as

$$L_{eff} = 2hf^2 / (D/2)^2 \quad (9)$$

Thus, by having the lens, we can have our first reading absolutely close to the surface. As the diameter of the AO-element is 5.2 mm, the lens in Fig. 1(b) might have a focal length of, for example, 55 mm, and the largest effective distance at which we can probe the object speckle field will be 44 mm.

4. Experiments using conventional free-space multiple plane setup

For the proposed technique to be feasible, the range of values for the effective distances is considered critical. In the free-space phase retrieval approach, the distance parameter is linked with two important aspects: 1) image sampling; and, 2) numerical aperture. According to the Nyquist detector sampling condition, the mean speckle size at the detector plane should be at least twice the detector pixel width (Δx). It is emphasized that, although the speckle intensity patterns are being subjected to this detector sampling condition, it is the change or variation in the intensity patterns between the adjacent planes that matters in the retrieval process [16]. The sampling condition simply states that a signal (here, the speckle patterns), which has f_{\max} as its highest spatial frequency, can be sufficiently represented using a detector with pixels that are $1/(2f_{\max})$ apart. It is further remarked that although sufficiency in the intensity sampling results in enhanced speckle patterns, it does not guarantee phasefront retrieval. It is the relationship between each pair of adjacent patterns that provides the means for the recovery of the phasefront. In other words, the manifestation of the phasefront (to be retrieved) is in the axial change in the speckle patterns, not in the patterns, *per se*.

The numerical aperture, on the other hand, characterizes the range of angles over which an optical system can accept light or its ability to gather light and resolve the specimen fine details, hence, sets the system resolution. During speckle recording, the effective numerical aperture is defined by the width of the camera sensor and the object-to-camera distance. In relation to the phase retrieval technique, the positions of the measurement planes, particularly the first plane, should be made sufficiently far from the object to satisfy the sampling condition. However, in order to maximize the numerical aperture and capture the high frequencies, the measurement planes should be positioned as near as possible to the object plane. These are opposing factors that are both critical, hence, should be balanced. It is emphasized that the speckle-based technique relies on, not a solitary measurement, but a plurality of measurements. Therefore, the individual measurements may violate the sampling condition; yet, the more important aspect of axial intensity variation may still be sufficiently

manifested. The favourable contributions of the axial intensity variation and the use of multiple patterns, in the retrieval process may dominate the effects of the violations of the sampling condition at each plane.

We conducted numerical and physical experiments to investigate two distance ranges using the conventional phase retrieval setup. The objective of the experiments is to assess the performance of the multiple plane phase retrieval technique at measurement distances that violate the Nyquist sampling condition. Figure 2 shows the schematic diagram of the setup used and the regions of interest where the measurement planes are located. As a way to relate the sample calculations obtained in the previous section, the values of the experimental parameters are chosen with reference to an effective distance of 44 mm. For the measurements in the non-Nyquist case ($L < Z_N$), the region involves axial distances that violate the Nyquist condition. The measurements for the Nyquist case ($L > Z_N$), involves distances that satisfy the Nyquist condition.

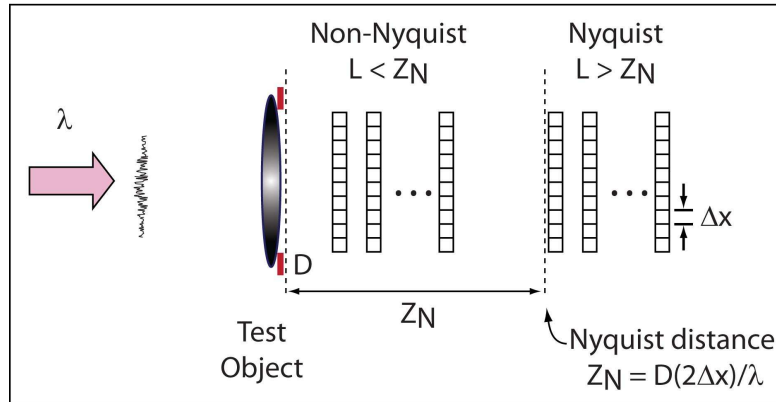


Fig. 2. Effects of recording the speckle field patterns at two measurement regions relative to the Nyquist sampling distance.

For both the numerical and physical experiments, the distance between planes (Δz) is 1 mm and the number of planes (N) is 20. The test object used is a positive lens ($f = 100$ mm) with an aperture diameter (D) of 3 mm. For the numerical experiment, the phase map is modulated by speckle noise to simulate the speckle illumination in the physical experiment. For the detector, Δx is 5.2 microns. The wavelength (λ) of the laser beam is 633 nm. Therefore, the Nyquist distance ($Z_N = 2\Delta x D/\lambda$) is 50 mm. For the non-Nyquist case, the first measurement plane is at $Z_0 = 20$ mm and the last plane is at $Z_{20} = 39$ mm. For the Nyquist case, the first measurement plane is at $Z_0 = 50$ mm and the last plane is at $Z_{20} = 69$ mm. During reconstruction, 3 iterations are employed. The phase maps for the two cases are plotted at the object plane. The fringe spacing on the phase map that can be resolved is used as a measure of the smallest phase structure that can be reconstructed for each of the two cases.

Figure 3 shows the results from the numerical simulations. Figure 3(a) shows the spherical phase distribution representing the test phase object with random noise. The intensity patterns of the propagated object wave at the two measurement regions are then sampled. For the Nyquist case, Fig. 3(b) is the unfiltered reconstructed phase map showing the spherical phase structures. The high frequency speckle phase may be removed using a low-pass filter. Comparing the phase maps in Fig. 3(a) and 3(b), the phase image correlation is 0.75. For the non-Nyquist case, the reconstructed phase map [Fig. 3(c)] displays similar spherical phase distributions. The correlation value obtained is slightly lower at 0.73. The acceptable reconstruction of the spherical phase structures, thus, indicates that the sampling condition is not a strict requirement in order for the multiple-plane phase retrieval technique to work. The object wavefront embodied in the sampled intensity patterns, despite violations of the Nyquist sampling condition, is still reconstructed with nominal decrease in the correlation of the phase

maps. Recording at a non-Nyquist range means that distances from the object and, in relation with the proposed AO-system, the effective distances may be kept at a minimum. This implies the feasibility of using DM's with small surface curvature heights which is the typical specification in faster and cheaper models. This also indicates the possibility of using an accessory lens with a shorter focal length, hence, a high numerical aperture.

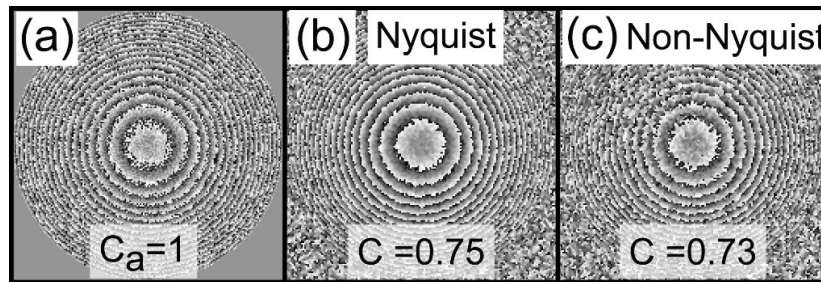


Fig. 3. Numerical simulations. (a) Initial phase at object plane. (b) and (c) are the reconstructed phase maps using intensity patterns recorded at Nyquist and non-Nyquist distances, respectively.

Figure 4 shows the experimental results using the conventional free-space multiple plane setup. For the Nyquist case, Fig. 4(a) shows the unfiltered spherical phase map at the object plane exhibiting 17 dark and bright rings. An inset depicts a zoomed-in section of the map with well-defined fringes. At the bottom portion of Fig. 4(a), a line scan shows the profile of the wrapped phase map demonstrating a good reconstruction. For the non-Nyquist case, Fig. 4(b) shows the phase map also displaying the spherical fringes. An inset also depicts a zoomed-in section of the phase map. The quality of the fringes in this section is considered acceptable. A line scan also shows the profile of the small fringes with fringe spacing in the range of 50 microns. The phase reconstruction shown in Fig. 4(b) proves that speckle measurements may be carried out at distances that do not conform with the Nyquist sampling condition, yet, still yield acceptable phase reconstruction for the test object used.

Here we have shown experimental and numerical proofs that the technique works despite using speckle data gathered over the non-Nyquist range. Possible contributory factors, that have been mentioned already, are the intensity variation afforded by the PDSF and the signal redundancy due to the fact that multiple measurements are used. As an additional factor, the inherent high contrast of the speckle patterns means that the test wavefront is adequately represented during the digitization process. Diminishing the effects of detector quantization, the high speckle contrast contributes in favor of the retrieval process, as well. Since quantization is not a serious issue in speckle intensity patterns, low bit-depth cameras may then be used. Images obtained at low-bit depth cameras have smaller file sizes, hence, could further facilitate for fast data acquisition [25].

As a further note on the role of the phase diffuser in the signal representation, sampling and retrieval, an analogous approach called the spread spectrum method has been employed in the field of telecommunications [26]. In the spread spectrum method, a new signal with a broad bandwidth is formed by purposely spreading, in the frequency domain, the original signal with a particular bandwidth. During its early development, the method was aimed for possible military applications particularly in resisting enemy efforts to jam the communications or in concealing the communications that were taking place. To determine and control the spreading pattern of the signal across an allotted bandwidth, generated pseudorandom patterns are used to encrypt the signal. In our optical case, the controlled randomization of the low-curvature test wavefront is facilitated by the nominally rough phase diffuser plate. The controlled spread of the wavefront results in a signal with a broader bandwidth (speckle patterns). A recorded speckle pattern, thus, efficiently represents the test wavefront. Combined with the intrinsic property of high speckle contrast, sufficient axial intensity variation, and signal redundancy within the volume speckle field samplings, the spread spectrum property of the speckle-based technique enhances the convergence rate of the

iterative algorithm. We believe these contributory factors to phase retrieval overcome the effects of the non-Nyquist speckle recordings.

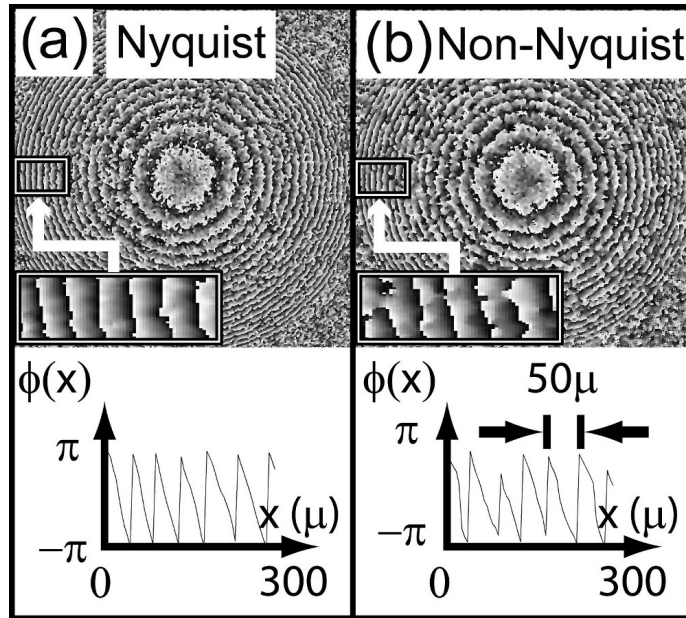


Fig. 4. Experimental results using conventional free-space setup. (a) and (b) are the reconstructed phase maps using speckle patterns recorded at Nyquist and non-Nyquist distances, respectively. The result in (b) demonstrates successful phase reconstruction of the test wavefront despite violations of the Nyquist condition during the speckle recording. This gives flexibility to the requirement of the surface height in the DM's in the proposed AO-system.

5. Summary and conclusions

We analyzed the extent and with what relation the insertion of a deformable mirror in the speckle-based PR method can replace the mechanical displacement of the recording detector. For the proposed AO-system, the values of the surface height and aperture diameter of the DM as well as the focal length of the accessory lens are calculated to determine the effective distances that can be probed within the object speckle field. The importance of the effective distance in the contexts of the Nyquist sampling condition and numerical aperture is investigated. Using the conventional free-space propagation approach, it was found that the detector planes may be located in a range that does not conform to the Nyquist sampling condition. The practical significance of this result, in relation to the proposed AO-scheme, is in terms of the possibility of using DM's with small surface heights, hence, fast devices at a cheaper cost. Finally, the proposed system seems to give the span in range measurements sufficient for a reasonable reconstruction via the PR method. The proposed setup allows measurements at high speed, hence, is adaptable to dynamically changing wave fields.

Acknowledgements

P. Almoro acknowledges the Office of the Chancellor, in collaboration with the Office of the Vice-Chancellor for Research and Development, of the University of the Philippines Diliman for funding support through the Outright Research Grant. The authors acknowledge the financial support from the Danish Council for Technology and Innovation under the Innovation Consortium CINO (Centre for Industrial Nano Optics).